The 200 MeV Bremsstrahlung Tagged Photon Beam at LNS-Sendai(I. Nuclear Physics)

The 200 MeV Bremsstrahlung Tagged Photon Beam at LNS-Sendai

A. Saito[1], M. Chiba[1], H. Kanda[1], R. Kimura[1], Y. Kobayashi[1], O. Konno[2], K. Maeda[1], H. Matui[2], H. Miyase[1], A. Miyamoto[2], T. Ohtsuki[2], T. Suda[1], T. Tamae[2], Y. Terasaki[2], T. Terasawa[2], H. Tsubota[1], M. Tsuruta[2] and H. Yamazaki[2]

[1]*Physics Department, Graduate school of Science, Tohoku University, Sendai 980-8578*
[2]*Laboratory of Nuclear Science, Tohoku University, Sendai 982-0826*
[3]*Institute of Physical and Chemical Research (RIKEN), 2-1 Hiragana, Wako 351-0098*

We describe the 200-MeV bremsstrahlung photon tagging system, which was installed in the experimental Hall-1 at the Laboratory of Nuclear Science, Tohoku University. This system produces tagged photons from high duty electron beams supplied by Stretcher Booster Ring. The tagged photon energies are over a range from 20% to 80% of the incident electron energy. We carried out commissioning to examine the performance of the tagged photon beams produced by the 198 MeV electron beam. We demonstrated that the tagged photons can be employed for photonuclear reaction experiments with a momentum resolution $\Delta p/p \sim 1\%$ at the tagged photon intensity $I \leq 5 \times 10^6$.

§ 1. Introduction

Real-photon induced nuclear reactions in an energy range from Giant Dipole Resonance (GDR) to near the pion threshold have extensively been studied at the Laboratory of Nuclear Science, Tohoku University (LNS-Sendai) using the Sendai STretcher Ring (SSTR) [1] and the photon tagging system [2]. The characteristic features in this energy region are excitations of the giant resonance (GR), the one-nucleon direct-knockout (DK) and the two-nucleon photon absorption due to the meson exchange current (MEC). During the experiments with SSTR, we have shown MEC plays a dominant role for the photon absorption process above GR [3-9]. Although we tried to investigate the two nucleon state through MEC by (γ, $2N$) reactions, sufficiently qualified data have not been obtained. In the Δ-resonance region, the (γ, $2N$) reactions have been studied at Tokyo [10,11] and Mainz [12]. They have shown that the photon energy dependence in the exclusive cross sections is scale to that of the deuteron photodisintegration cross section. Consequently, the photon absorption by the two nucleons is thought to dominate the photonuclear reaction process above GR and can be applied to study the two nucleon states in nuclei.

The facility was once closed during the period of 1994 − 1998 to upgrade from SSTR to Stretcher Booster Ring (STB). The functions of STB are the pulsed beam stretcher, the energy booster and the beam accumulator. The real-photon induced experiments became to be carried out with the maximum electron energies of 0.3- and 1.2-GeV using the stretcher and the booster-accumulation mode, respectively.

In order to use the extracted 0.3-GeV stretched beam for the real-photon induced nuclear reaction experiments, we constructed a new beam line and a upgraded photon tagging system. This article reports the performance of the new beamline and the photon tagging system, and the representative results of the tagger commissioning.

§ 2. Experiment

2.1 LNS/STB Tagging system

The electron beams stretched by STB are delivered to the experimental Hall-1 through a newly constructed beam transport line called BL-V. The schematic BL-V layout is shown in Fig.1, together with STB and the experimental Halls. BL-V consists of three straight sections and two 90° deflecting system. The beams are transported by achromatic designed components with four dipole-magnets, four pairs of quadrupole-magnets and five beam-steering coils. Brass collimators were placed at the first and second straight section. The beamline length from STB to the tagger is about 80-m long. The beam spot size is monitored at the middle of second straight section, and the bremsstrahlung target position with photo-luminescence plates (ZnS). A plastic scintillation counter located just behind the second quadrupole-magnet, which is used to monitor the loss and the time structure of the electron beam. The beam ducts are made of 50 mm-diameter aluminum tube. They are evacuated by four ion pumps and three turbo-molecular pumps to a vacuum presser of $\sim 10^{-5}$ Pa.

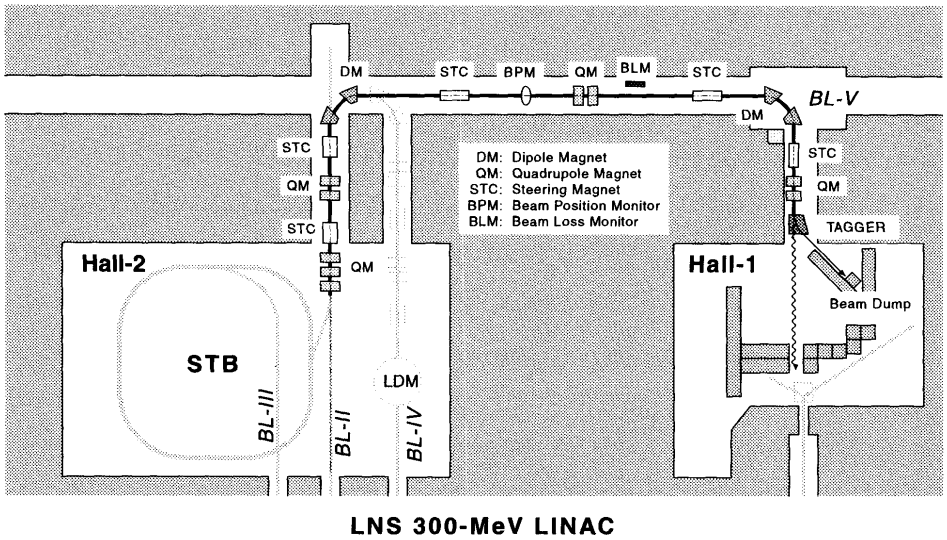

Fig.1. Schematic layout of BL-V. Gray lines show beam lines and STB. Solid line is BL-V.

As shown in Fig.2, the photon tagging system is located at the end of BL-V in Hall-1. The electron beams produce photons in a bremsstrahlung target placed at the entrance of the tagger. The photons irradiate the nuclear reaction target placed in Hall-1. The primary electron beam is stopped in the well-shielded beam dump. A thin-wall chamber, which is placed in front of the beam stopper, is used to monitor the beam intensity.

2.2 Tagging spectrometer

The tagging spectrometer is composed of a bremsstrahlung radiator, a dipole magnet and electron counters. As shown in Fig.2, the incident electrons are impinged on a target in a radiator box, where

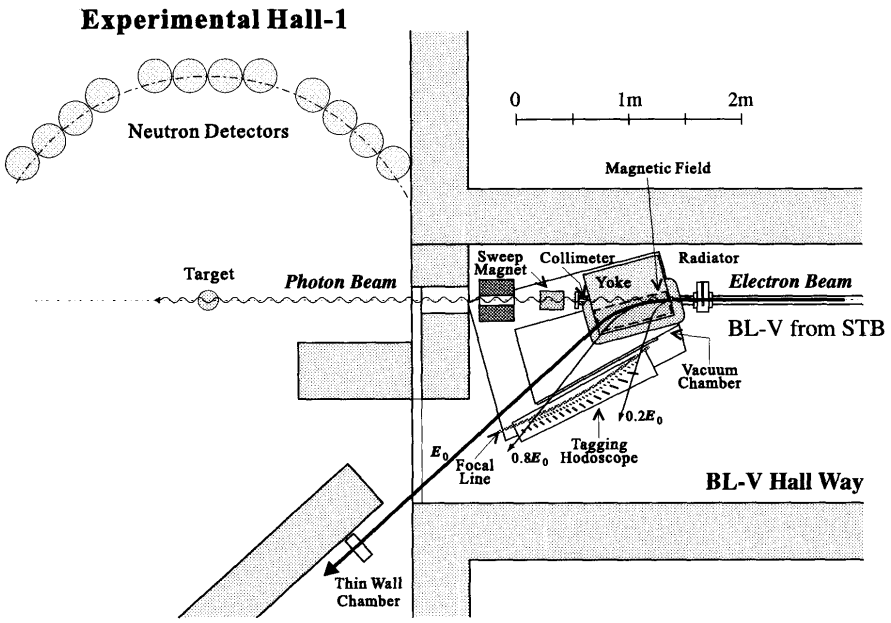

Fig.2. Layout of the photon tagging system and the neutron detector setup.

three bremsstrahlung radiator; a gold (3 μm), a platinum (10 μm) and an aluminum (80 μm) foils, and a ZnS beam monitor, are mounted on a rotatable device.

The tagged photon energy E_γ is determined as,

$$E_\gamma = E_0 - E_e - E_{recoil}, \quad (1)$$

where E_0 and E_e is the incident and outgoing electron energy, respectively. Since the transferred energy to the recoil nucleus E_{recoil} is negligibly small, the tagged photon energy E_γ is uniquely determined by E_0 and E_e, The incident electron energy E_0 is controlled by the STB operation and the BL-V condition. The energy of the post bremsstrahlung recoil-electron E_e is analyzed in a magnetic field. The magnetic field is generated by a simple rectangular-pole-shape magnet with 50 mm gap. This magnet allows a broad momentum acceptance, and puts the position of the focal plane far away from the magnetic field. The second order matrix calculation of the electron trajectories showed the momentum resolution $\Delta p/p \sim 1 \times 10^{-3}[\mathrm{mm}^{-1}]$ at the middle of the focal plane.

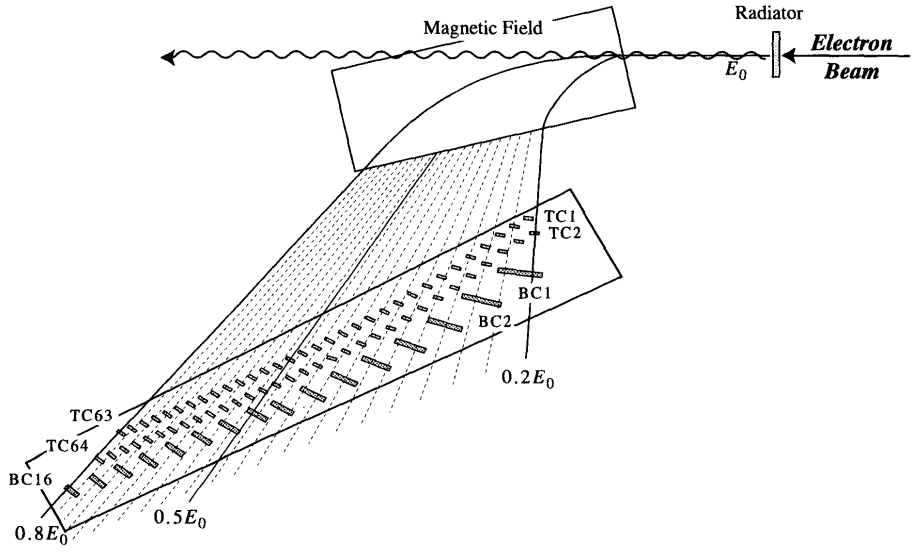

Fig.3. Bremsstrahlung recoil-electron trajectories in the tagger and the array of tagging and tagging-backup counters.

A plastic-scintillator hodoscope was used for the focal plane detector. It consists of 64-channnel tagging counters (TC) and 16-ch tagging-backup (BC) counters covered the energy range from 0.2 to 0.8 E_0. The widths of TC vary from 6.6 to 18.3 mm to achieve equal momentum acceptance of $\Delta p / p_0 \sim 9.3 \times 10^{-3}$, where p_0 is the incident electron momentum. When the higher energy electrons than 250 MeV become available at BL-V, the tagger energy range will be $E_\gamma^{MAX} = E_e - 30$ MeV to $E_\gamma^{MIN} = E_e - 130$ MeV keeping the energy resolution $\Delta E_\gamma \sim 1.5$ MeV. As shown in Fig.3, 32 TCs (F-TC) are located on the focal line of the tagging magnet and another 32 TCs (B-TC) placed just behind them. The horizontal beam-expanse at the B-TC position is calculated to be less than 0.5 mm, which is small enough compared with the position resolution.

The array of BC is used to reduce the accidentals that mainly come from electron hits of the beam line components. Sixteen units of a BC and four TCs are placed on the recoil-electron trajectories. The coincidence between a BC and a corresponding TC signal restricts the electron trajectory and efficiently, and gets rid of backgrounds.

2.3 Data acquisition

The tagger signals are processed by sixteen 4 channel Quad-Tag Modules (QTM). Each QTM accepts independent four linear signals from TC. After the TC signals are amplified and discriminated, they are strobed by a timing signal from the corresponding BC. Each QTM channel produces two strobed, one discriminated and one delayed (106 ns)-strobed TC timing signals. There is a logical sum-out [$\Sigma 4$] of four strobed TC signals in QTM. As shown in Fig.4, the trigger signal of the tagger side is,

$$[\Sigma 64] = \sum_{i=1}^{16} [\Sigma 4]_i \tag{2}$$

$$= \sum_{i=1}^{16} \sum_{j=1}^{4} [TC]_{4i-j+1} \tag{3}$$

where $[\Sigma 4]_i$ is the i-th QTM strobed sum-out.

In Fig.5, a sample circuit diagram for the (γ, np) experiment using liquid scintillation counters (LS) for neutrons and a multilayer range telescope (RT) for protons. The event trigger signals from LS and RT side are obtained by the coincidence between the timing signals from LS and RT. The first trigger signals for the data taking are generated by the event trigger signals in coincidence with [$\Sigma 64$] from the tagger as,

$$[\mathrm{ET}] = [\Sigma 64] \otimes ([\mathrm{LS}] \otimes [\mathrm{RT}]) \otimes [\overline{\mathrm{veto}}], \tag{4}$$

where $[\overline{\mathrm{veto}}]$ is any veto signals from the cletectors and the accelerator.

We use a CAMAC+PC/LINUX system to take online data. As shown in Fig.6, the data encoded in CAMAC modules are collected through CC7700 CAMAC crate controller (CC) and ISA-bus interface. The data taking software, which was developed under the LINUX operating system, collects, analyzes and records the raw data.

When the collector receives a LAM signal from CAMAC, it starts to transfer the raw data from CAMAC. The recorder writes the forwarded data from the collector on the shared memory and stores them on the DVD-Ram drive. The analyzer displays the data on the monitor screen and refreshes the

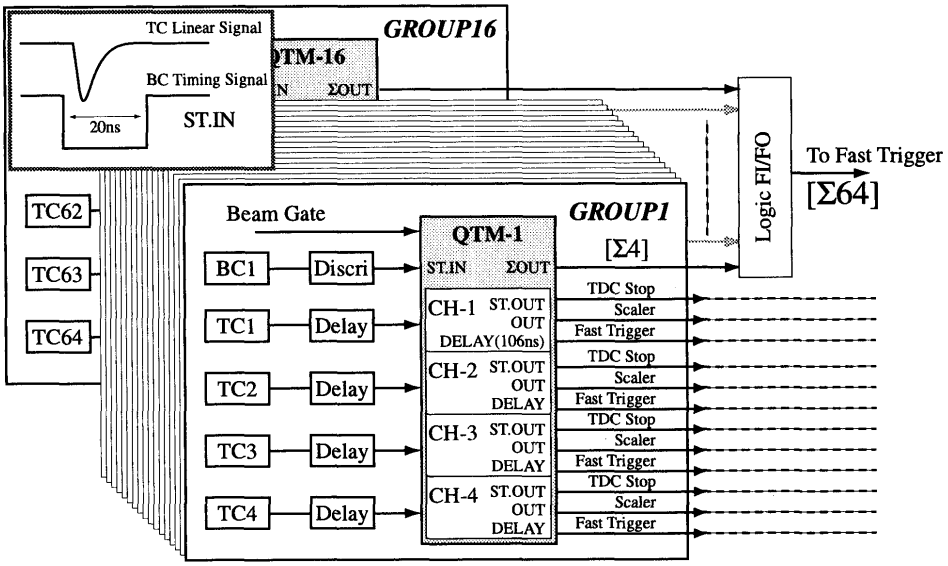

Fig.4. Schematic diagram of the tagger electronics.

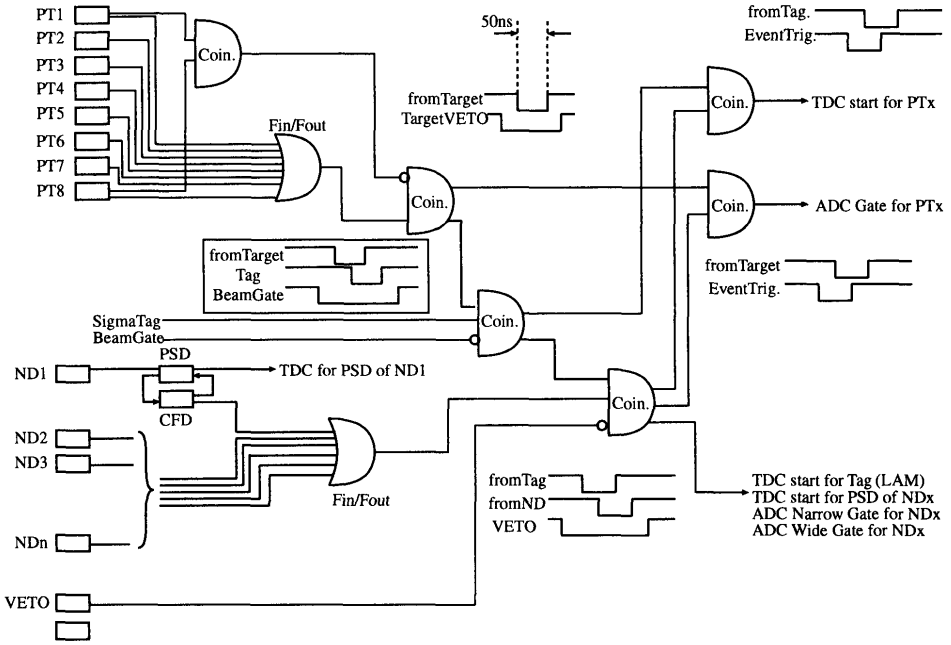

Fig.5. A typical circuit diagram for the (γ , np) experiment.

screen every few seconds. These processes are controlled by the process controller, which is controlled via a visual interface panel displayed on the monitor screen.

§ 3. Tagger Commissioning

The performances of the tagging system were examined by offline tests and commissioning experiments using a 198 MeV electron beam from LNS/STB. In the first stage of commissioning, relative timings among [TC] and [TC-BC] were verified. After the tuning of tagger counters, we measured several performance data of the tagging system such as the off/on ratio, the tagging efficiency and the count rate dependence.

3.1 Radiator off/on ratio

In addition to the electrons from the radiator, the background radiations hit TC and BC. Their

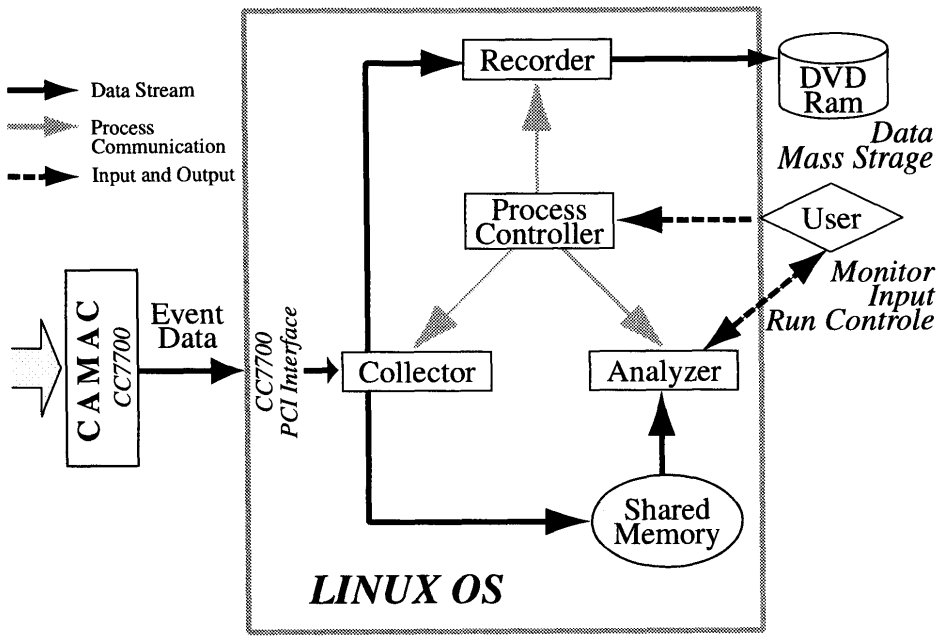

Fig.6. Flow diagram of online data taking system. Event data from the CC7700 crate controller and PCI-interface are processed by a online software under the LINUX Operation System. The online software consists of a collector, an analyzer, and a recorder and a process controller. The raw and histogram data are mass-storaged on DVD ram-disk.

main contributions are the room background from the transport line and the electron beam dump, and the hits of electron beam halo on the radiator holder. In order to estimate the background, we measured the ratio of each TC counting rate with (ON) to without (OFF) the radiator. In Fig.7, we show TC counts of ON (A) and OFF (B), and the ratio of OFF to ON (C), where the 3 μm Au target (10^{-3} radiation length) was used. As shown in Fig.7(C), the average counts ratio of OFF to ON is less than 5%. Although this value must be reduced by the more careful tunings of the STB and BL-V parameters, it might be endured to carry out the photonuclear reaction experiments.

3.2 Tagging efficiency

The tagging efficiency is defined as the ratio of the photon number to the electron counts. We employed a lead glass Cherenkov detector (20 radiation length) to count the tagged. The tagging efficiency of i-th counter is obtained as,

$$\varepsilon_i = \frac{N_i^{TB}(\text{on}) \otimes N^{C}(\text{coin.}) - N_i^{TB}(\text{on}) \otimes N_i^{C}(\text{acc.})}{N_i^{TB}(\text{on}) - N_i^{TB}(\text{off})} , \qquad (5)$$

where N are the counts of rm [TC] $\otimes$ [BC] (TB) and the Cherenkov counter (C) with the conditions of radiator [on] and [off], and coincidence [coin] and accidental [acc.] events. The obtained photon tagging efficiency is shown in Fig.8, where the open circles are experimental result and the closed circles with error bar represent the results of a GEANT simulation.

3.3 Counting rate dependence

The counting rate dependence of the tagging efficiency must be very important to determine the absolute values of the cross section. Since the stability of the D.F. strongly depends on the STB condition, we have to monitor the fluctuation of the D.F. during the measurements to correct for the

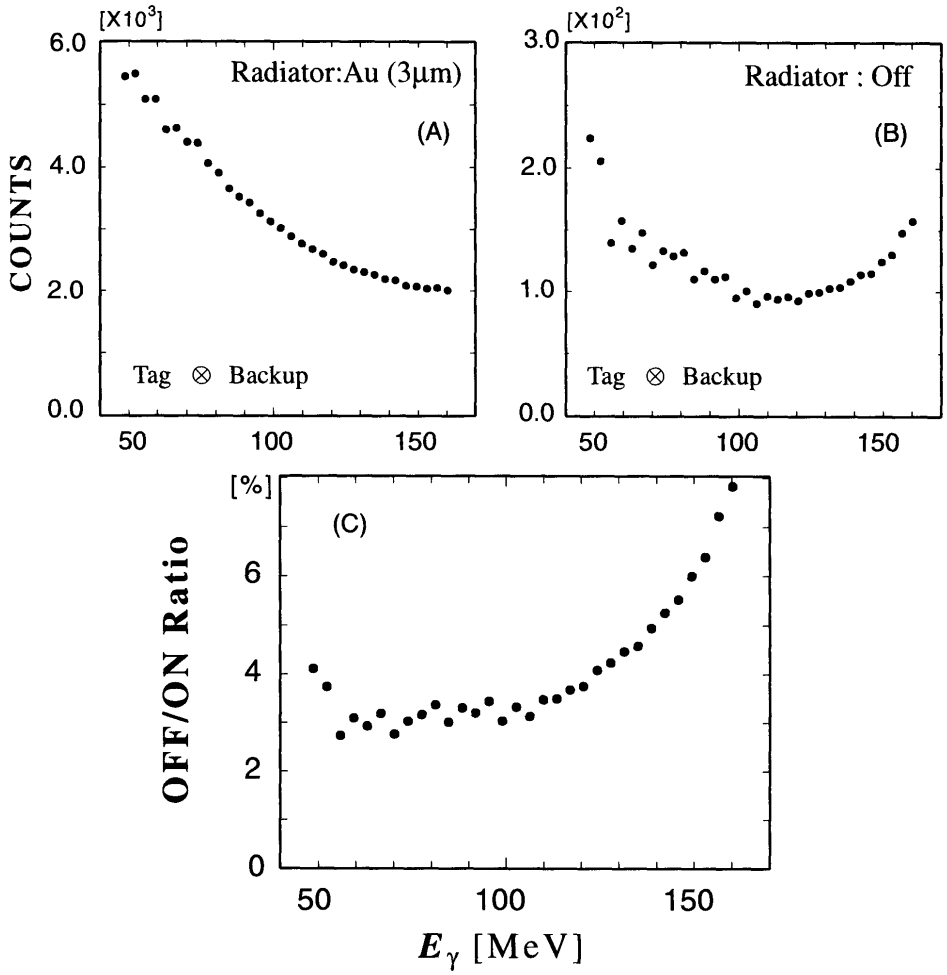

Fig.7. [TC] ⊗ [BC] counts of each tagging counters. (A) and (B) are radiator-on with 3 μm Au radiator and radiator-off, respectively. (C) shows the counts ratio of the radiator-off to radiator-on. These figures show the data for the even numbered tagging counters placed on the focal line.

tagging efficiency. The relation between the D.F. and the counting rate is,

$$\text{D.F.} = \frac{N_i \cdot N_j \cdot \tau}{N_{acc}}, \qquad (6)$$

where N_i and N_j are the counting rate of any two TCs, N_{acc} is the accidental coincidence rate between $[TC]_i$ and $[TC]_i$ with the resolving time of τ. Unfortunately, the average beam D.F. was 20-30% during the tagger commissioning. We found the $[\Sigma 64] \sim 1.4 \times 10^6$ at the 100% equivalent D.F. is the maximum photon number without any serious corrections for the tagging efficiency.

§ 4. Conclusion

The LNS 200 MeV bremsstrahlung photon tagging system was installed in LNS/Hall-1. We have shown the required performances are satisfied to carried out any real-photon experiments in the photon energy range between GR and Δ-resonance. We need an additional STB tune to improve D.F. for the planned ^{40}Ca(γ, n) and ^{12}C(γ, np) experiments.

When the STB operation become to keep up with the slow extraction combined with the booster mode, the high-duty electron beam can be transported to the Hall-1 with a minor modification of BL-V.

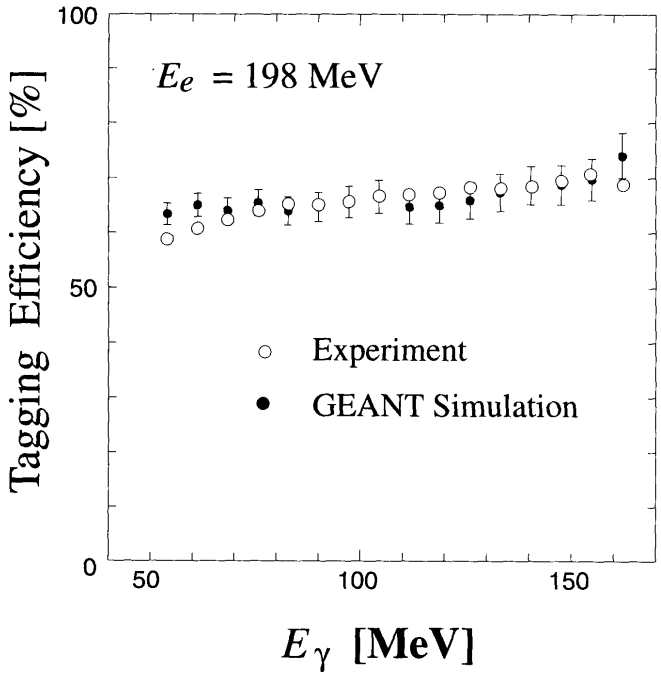

Fig.8. Photon tagging efficiency

The summary of the present tagger commissioning and the typical parameters of the elec-tron beams and the LNS photon tagging system is tabulated in Table 1 . As shown in the table, the high-resolution photon beams can be use for the photonuclear reaction experiments above the Δ-resonance using the presently developed photon tagging system.

This article is an interim report for the tagger and BL-V commissioning that were carried out in accordance with the LNS-proposal #2273.

Table 1. Parameters of photon tagging system at BL-V.

	Present Commissioning	Typical Stretcher Mode	Typical Booster Mode
Electron energy (E_0)	198 MeV	250 MeV	500 MeV
Duty factor	~30%	80%	80%
Tagging range	40-160 MeV	$0.2E_0$-$0.8E_0$	370-470MeV
Tagging resolution	1.8 MeV	$9.3\times10^{-3}E_0$	1.5 MeV
Tagging efficiency	0.65	0.7	0.8
Tagged photon rate	1.4×10^6 s^{-1}	5×10^6 s^{-1}	5×10^6 s^{-1}

References

[1] T. Tamae, M. Sugawara, K. Yoshida, O. Konno, T. Sasanuma, M. MutoY. Shibazaki, T. Tanaka, M. Hirooka, K. Yamada, T. Terasawa, S. Ura-sawa, T.Ichinohe, S. Takahashi, H. Miyase, Y. Kawazoe, S. Yamamoto and Y. Torizuka: Nucl. Instr. and Meth. **A264** (1988) 173.

[2] T. Terasawa, K. Mori, Y. Fujii, T. Suda, I. Nomura, O. Konno, T. Ichinohe, Y. Torizuka, K. Maeda, P.D. Harty, G.J. O'Keefe, M.N. Thompson: Nucl. Instr. and Meth. **A248** (1986) 429.

[3] P.D. Harty, M.N. Thompson, G.J. O'Keefe, R.P. Rassool, K. Mori, Y. Fujii, T. Suda, I. Nomura, O. Konno, T. Terasawa, Y. Torizuka: Phys. Rev. C**37** (1988) 13.

[4] T. Suda, O. Konno, I. Nomura, T. Suzuki, T. Terasawa, Y. Torizuka, J. Yokokawa, K. Maeda, J. Eden, G.O'Keefe, R. Rassool, M. Thompson, J. Kim: J. Phys. Soc. Jpn. **57** (1988) 5.

[5] J. Yokokawa, O. Konno, I. Nomura, T. Suda, T. Suzuki, T. Terasawa, Y. Torizuka, K. Maeda, J. Eden, D. McLean and M. Thompson: J. Phys. Soc. Jpn. **57** (1988) 6955.

[6] J.A. Eden, G.J. O'Keefe, R.P. Rassool, D.J. McLean, M.N. Thompson, T. Suda, I. Nomura, J. Yokokawa, O. Konno, T. Terasawa, Y. Torizuka: Phys. Rev. C**44** (1991) 753; Erratum Phys. Rev. C**46** (1992) 385.

[7] D.A. Sims, S. Karataglidis, G.J. O'Keefe, R.P. Rassool, A.D. Bates, M.N. Thompson, S. Ito, H. Matsuyama, S. Sazaki, O. Konno, T. Terasawa, T. Suda, K. Maeda: Physical Review C**45** (1992) 479.

[8] S. Ito, K. Maeda, T. Fukuda, O. Konno, T. Suda, M. Takeya, T. Terasawa: Nucl. Instr. and Meth. **A354** (1995) 475.

[9] K. Mori, P.D. Harty, Y. Fujii, O. Konno, K. Maeda, I. Nomura, G.J. O'Keefe, J. Ryckebusch, T. Suda, T. Terasawa, M.N. Thompson, Y. Torizuka: Phys. Rev. C**51** (1995) 2611.

[10] T. Emura, I. Endo, S. Endo, H. Itoh, S. Kato, M. Koike, K. Maeda, T. Maki, S. Maruo, K. Maruyama, Y. Murata, K. Niki, C. Rangacharyulu, A. Sasaki, T. Suda, Y. Sumi, Y. Wada, K. Yoshida: Phys. Lett. **286B** (1992) 229.

[11] K. Maruyama, K. Niki, Y. Sumi, T. Emura, I. Endo, S. Endo, H. Itoh, S. Kato, M. Koike, K. Maeda, T. Maki, Y. Murata, C. Rangacharyulu, A. Sasaki, T. Suda, Y. Wada, K. Yoshida, and the TAGX Collaboration: Phys. Lett. **393B** (1997) 295.

[12] I.J.D. MacGregor, T.T-H. Yau, J. Ahrens, J.R.M. Annand, R. Beck, D. Branford, P. Grabmayr, S.J. Hall, P.D. Harty, T. Hehl, J.D. Kellie, T. Lamparter, M. Liang, J.A. MacKenzie, S. McAllister, J.C. McGeorge, R.O. Owens, J. Ryckebusch, M. Sauer, R. Schneider, D.P. Watts: Phys. Rev. Lett. **80** (1998) 245.

[13] J.C. McGeorge, I.J.D. MacGregor, S.N. Dancer, J.R.M. Annand, I. Anthony, G.I. Crawford, S.J. Hall, P.D. Harty, J.D. Kellie, G.J. Miller, R.O. Owens, P.A. Wallace, D. Branford, A.C. Shotter, B. Schoch, R. Beck, H. Schmieden and J.M. Vogt: Phys. Rev. C**51** (1995) 1982.